



Article

Rotary Friction Welding of Inconel 718 to Inconel 600

Ateekh Ur Rehman ^{*}, Yusuf Usmani, Ali M. Al-Samhan and Saqib Anwar 

Department of Industrial Engineering, College of Engineering, King Saud University, Riyadh 11451, Saudi Arabia; yusmani@ksu.edu.sa (Y.U.); asmhan@ksu.edu.sa (A.M.A.-S.); sanwar@ksu.edu.sa (S.A.)

* Correspondence: arehman@ksu.edu.sa; Tel.: +966-1-1469-7177

Abstract: Nickel-based superalloys exhibit excellent high temperature strength, high temperature corrosion and oxidation resistance and creep resistance. They are widely used in high temperature applications in aerospace, power and petrochemical industries. The need for economical and efficient usage of materials often necessitates the joining of dissimilar metals. In this study, dissimilar welding between two different nickel-based superalloys, Inconel 718 and Inconel 600, was attempted using rotary friction welding. Sound metallurgical joints were produced without any unwanted Laves or delta phases at the weld region, which invariably appear in fusion welds. The weld thermal cycle was found to result in significant grain coarsening in the heat affected zone (HAZ) on either side of the dissimilar weld interface due to the prevailing thermal cycles during the welding. However, fine equiaxed grains were observed at the weld interface due to dynamic recrystallization caused by severe plastic deformation at high temperatures. In room temperature tensile tests, the joints were found to fail in the HAZ of Inconel 718 exhibiting good ultimate tensile strength (759 MPa) without a significant loss of tensile ductility (21%). A scanning electron microscopic examination of the fracture surfaces revealed fine dimpled rupture features, suggesting a fracture in a ductile mode.

Keywords: superalloys; dissimilar welding; friction welding; microstructure; mechanical properties



Citation: Rehman, A.U.; Usmani, Y.; Al-Samhan, A.M.; Anwar, S. Rotary Friction Welding of Inconel 718 to Inconel 600. *Metals* **2021**, *11*, 244. <https://doi.org/10.3390/met11020244>

Academic Editor: Yutaka S. Sato

Received: 21 December 2020

Accepted: 28 January 2021

Published: 1 February 2021

Publisher's Note: MDPI stays neutral with regard to jurisdictional claims in published maps and institutional affiliations.



Copyright: © 2021 by the authors. Licensee MDPI, Basel, Switzerland. This article is an open access article distributed under the terms and conditions of the Creative Commons Attribution (CC BY) license (<https://creativecommons.org/licenses/by/4.0/>).

1. Introduction

Technological advancements in various industrial sectors have placed a high demand for materials with superior performance in harsh working conditions. Although ceramic materials display excellent resistance to environmental degradation, they are not suitable for use in most of the structural applications because of their low fracture toughness and poor performance under tensile loading conditions. On the other hand, refractory metal alloys show impressive high temperature strength but suffer from poor oxidation resistance. Hence, nickel-based superalloys have emerged as the primary choice for structural applications at elevated temperatures because of their good high temperature mechanical properties and excellent environmental resistance [1].

Several Ni-based superalloys based on a solid solution and precipitation strengthening have been developed over the years to suit a wide range of applications from gas turbines to high temperature furnace accessories. These alloys find extensive use in rocket engines, aero engines and the industrial power turbine [2]. Inconel 600 is a solid solution strengthened Ni-based superalloy with as much as 72% (wt.) nickel [3,4]. The alloy finds extensive use in pressurized water reactors. On the other hand, Inconel 718 is a precipitation strengthened Ni-based superalloy. Strengthening in this alloy is primarily due to the precipitation of γ'' (Ni_3Nb) while an amount of γ' ($\text{Ni}_3(\text{Al,Ti})$) is also present [2–5]. Inconel 718 shows excellent formability, weldability and can perform well over a wide temperature range from sub-zero temperatures to 650 °C [6]. Employing different materials with specific properties in different locations of a single fabricated component is economical and effective in terms of its operational performance. However, the fabrication of such multi-material components calls for dissimilar metal joining. In fact, with the availability of more and more new

materials with diverse properties, dissimilar welding is assuming greater significance and use in various industrial sectors [7].

In conventional fusion welding, it is often difficult to match the properties of the weld metal and the heat affected zone (HAZ) with the optimized properties of the base metal achieved through complex thermo-mechanical treatments. The as-cast microstructure of the weld metal and undesirable microstructural changes in the HAZ often limit the performance of a fusion welded joint. Moreover, in fusion welds, the segregation of alloying elements during solidification often results in the formation of some undesirable brittle intermetallic phases. For example, pulsed Nd-YAG laser welds in Inconel 718 were reported to show inferior tensile properties in a direct aged condition due to the presence of an Nb-rich Laves phase in the weld fusion zone [8]. In γ'' strengthened nickel-based superalloys, the segregation of Nb and other alloying elements led to Laves formations during the terminal stages of the solidification. The presence of a low melting Laves phase in Inconel 718 castings is known to cause HAZ liquation cracking (microfissuring) during fusion welding [9]. Most of the fusion welding problems, such as solidification and subsequent segregation effects, can be avoided by resorting to solid-state welding techniques such as rotary friction welding. Friction welding involves intense frictional heating between the surfaces that are in relative motion, which results in a severe plastic deformation of the materials at the weld interface. The mechanical intermixing of the materials caused by severe plastic deformation and enhanced diffusion due to high temperatures result in a strong metallurgical bonding at the weld interface [10]. It was reported that friction welds in Inconel 718 were free from a Laves phase and other weld defects, which invariably form in fusion welds [11,12]. The friction welds were reported to show a fine grained structure at the weld interface and responded well to post-weld direct aging treatment. Smith et al. have reported that the grain boundary liquation and subsequent low melting grain boundary phase formation were not observed in the Inconel 718 welds prepared by a linear friction welding technique [13]. This was attributed to the lower peak temperatures during the friction welding and small precipitate sizes in the parent alloys. Grain refinement as a result of the dynamic recrystallization resulted in the significant increase in the hardness at the weld interface compared with the base metals. Dynamic recrystallization and the grain boundary sliding play a competitive role in the development of the weld metal grain structure during friction welding [14]. Grain boundary sliding due to the finer grain size in the recrystallized weld metal has resulted in a lower axial force during rotary friction welding of Inconel 718 alloy tubes. In another study, defect free dissimilar Inconel 600 and 304 L friction welded joints were prepared from cylindrical rods of a 12 mm diameter [15]. The dissimilar 600–304 L friction welded joints displayed no significant drop in tensile strength from room temperature to 450 °C while a drastic drop in the tensile strength was observed above 450 °C. All of the specimens failed in the base metal during the tensile testing indicating the soundness of the welds. In this work, dissimilar welding of Inconel 718 to Inconel 600 was attempted using rotary friction welding. The weld microstructural characteristics were investigated in detail. Room temperature tensile tests were also performed on the welds. To the best of the authors' knowledge, dissimilar welding of Inconel 718 to Inconel 600 has not been tried before using friction welding.

2. Experimental Techniques

Inconel 718 and Inconel 600 rods (20 mm diameter and 100 mm length) in solution treated and mill annealed conditions, respectively, were used in the present investigation. The chemical compositions of these alloys are listed in Table 1. The base metals were face turned and cleaned with acetone before friction welding to remove surface oxides and other contaminants. Friction welding experiments were conducted on a continuous drive rotary friction welding machine (ETA Technology, Bangalore, India) of 150 kN capacity. The Inconel 718 was held in the non-rotating vice and the Inconel 600 in the rotating chuck. Theoretically, there should not be any difference on which side, rotating or non-rotating, a particular alloy is held but in a practical sense it does have a minor effect. The rotating side

of the base alloy, because of the forced convection of the ambient air around its surface, cools down faster compared with the other alloy that remains stationary. The faster cooling in turn could affect the microstructure in the rotating alloy depending on its sensitivity to such a minor temperature drop. The friction welding experimental procedure has been detailed elsewhere [16]. The welding parameters are listed in Table 2.

Table 1. Chemical composition of the Inconel 718 and Inconel 600.

Alloy/wt. %	Ni	Cr	Nb	Mo	Ti	Al	C	Fe	Others
Inconel 718	52.5	19	5.7	3	0.9	0.5	0.08	Bal.	0.18 Cu
Inconel 600	72	16	-	-	-	-	0.15	Bal.	0.2 Cu, 0.15 Si, 0.5 Mn

Table 2. Friction welding parameters.

Friction Pressure (MPa)	Friction Time (s)	Welding Speed (rpm)	Upset Pressure (MPa)	Upset Time (s)
60	3	1500	80	6

The base metals and the welded joints were suitably sectioned, polished using standard metallographic techniques and electrolytically etched using a solution consisting of 10 gm oxalic acid and 90 mL distilled water. Electrolytic etching was carried out at 3 V for 15 s. A microstructural examination at a low magnification was carried out using a Nikon SMZ745T stereo microscope (Nikon Instruments Inc., New York, NY, USA). Microstructural studies at high magnifications were carried out using a TESCAN VEGA 3LMV scanning electron microscope (SEM, TESCAN USA, Warrendale, PA, USA) equipped with energy dispersive spectroscopy (EDS) (Oxford Instruments, Abingdon, UK). The accelerating voltage employed during the SEM investigation was 20 kV. Grain size measurements were carried out by analyzing corresponding optical and SEM micrographs using ImageJ software. Vickers microhardness measurements were carried out across the weld region using a diamond pyramid indenter (Shimadzu, Tokyo, Japan) under a load of 50 g applied for 15 s. The center to center distance of the indentations during the hardness measurements was 0.5 mm. Transverse weld specimens of 25 mm gauge length and 4 mm diameter were machined from the friction welded rods. Tensile tests were carried out on base metal and weld specimens using a servo hydraulic testing machine (Instron, Norwood, MA, USA) at a constant displacement rate of 0.5 mm/min. Tensile tests were performed as per the ASTM-E8-04 standard specimen configuration. An average of the test results obtained from the three specimens was taken during the hardness and tensile investigations of the samples. Fracture surfaces of the failed tensile specimens were examined under SEM using a secondary electron imaging mode.

3. Results and Discussion

3.1. Microstructure

Optical and scanning electron micrographs of Inconel 718 and Inconel 600 base metals are shown in Figure 1. The optical micrograph (Figure 1a) of Inconel 718 reveals fine equiaxed grains with an average grain size of $24.5 \pm 11 \mu\text{m}$. The Inconel 718 contained some coarse second phase particles predominantly at the grain boundaries (Figure 1c), which were identified based on EDS analysis as MC carbides containing Nb and Ti (Figure 1e). These MC carbides remained undissolved during solution treatment and could restrict grain growth [2,17]. The Inconel 600 showed a fully equiaxed grain structure with an average grain size of $38.5 \pm 22 \mu\text{m}$ (Figure 1b). An EDX analysis revealed that the Inconel 600 contained some TiN second phase particles, which were present both within the grains and at the grain boundaries (Figure 1d,f). Similar TiN second phase particles in the Inconel 600 microstructure have also been reported elsewhere [4].

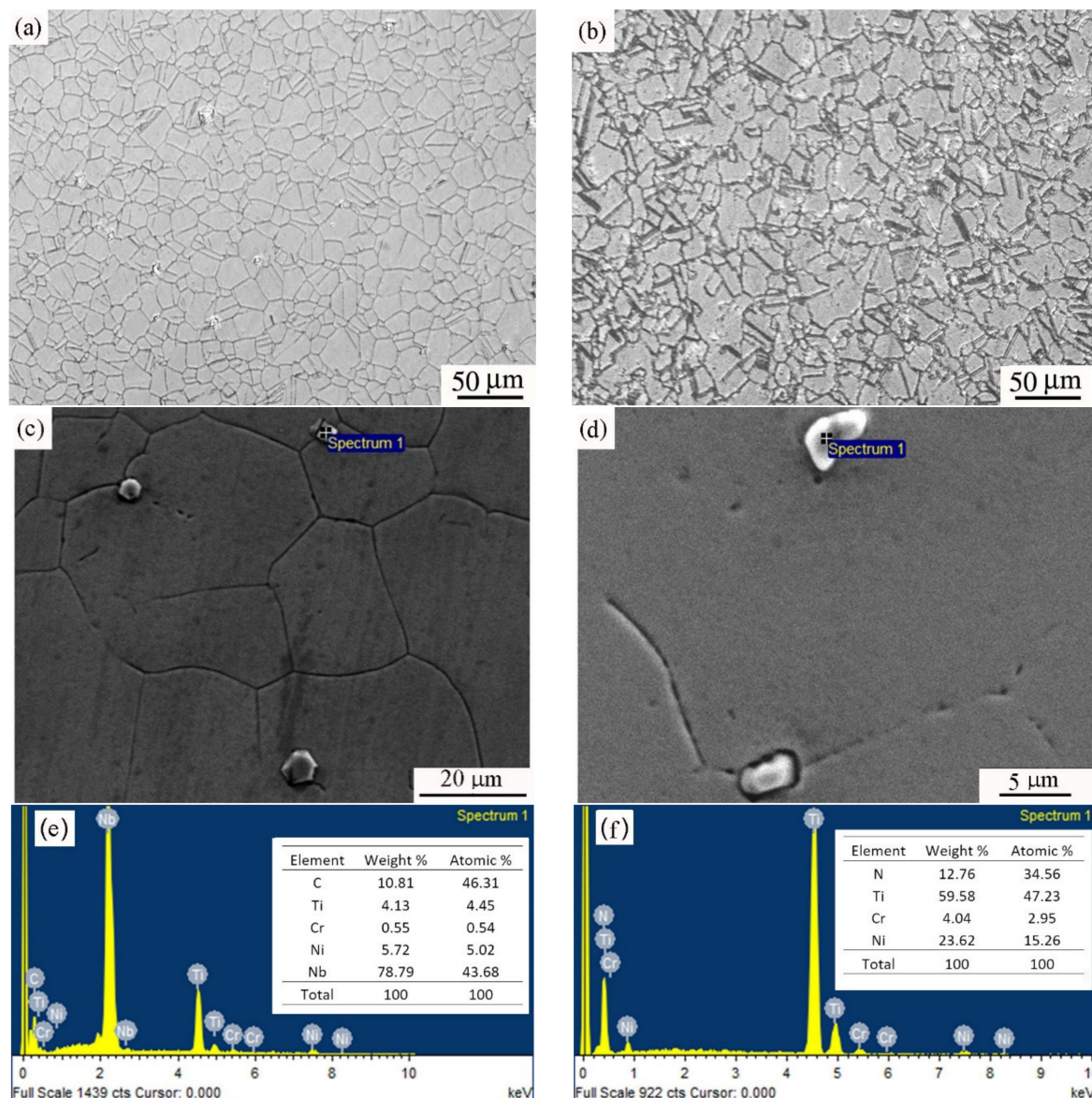


Figure 1. Optical and scanning electron micrographs of Inconel 718 (a,c) and Inconel 600 (b,d). (e,f) show EDS spectra obtained from second phase particles present in Inconel 718 and Inconel 600, respectively.

A macrograph of the weld (longitudinal section) is shown in Figure 2. No macroscopic defects were observed at the weld interface. A mechanical intermixing zone consisting of very fine recrystallized grains was observed at the weld interface. Next to this zone, some coarse grains were observed in the HAZ on either side.

The HAZ microstructures of Inconel 718 and Inconel 600 are shown in Figure 3a,b, respectively. The average grain sizes in the HAZ of Inconel 718 and of Inconel 600 were found to be $359 \pm 127 \mu\text{m}$ and $268 \pm 86 \mu\text{m}$, respectively. During friction welding, intense heating occurs at the weld interface and high temperatures (close to $0.8 T_m$) are attained. As a result, some grain growth occurs in the HAZ [18]. It may be noted that Inconel 718 showed more prominent grain coarsening in the HAZ compared with the Inconel 600. During friction welding, the thermal cycles experienced by the materials placed on the stationary and rotating sides can be significantly different (in this work, Inconel 718 was placed on the stationary side). Furthermore, the width of the HAZ and the level of grain coarsening in the HAZ are also dependent on the base metal thermal conductivity as well as the presence or absence of any grain boundary pinning second phases [19]. These factors explain why the HAZ grain coarsening was more prominent on the Inconel 718 side.

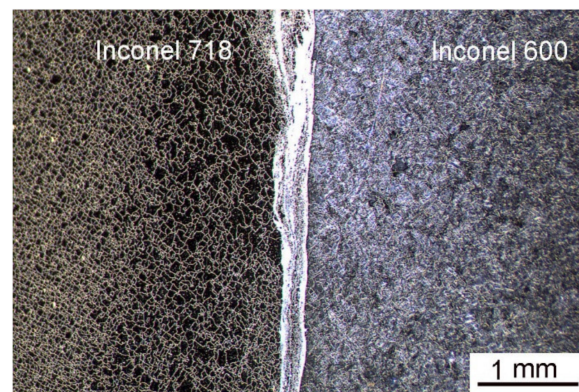


Figure 2. Macrograph of Inconel 718/Inconel 600 dissimilar friction weld.

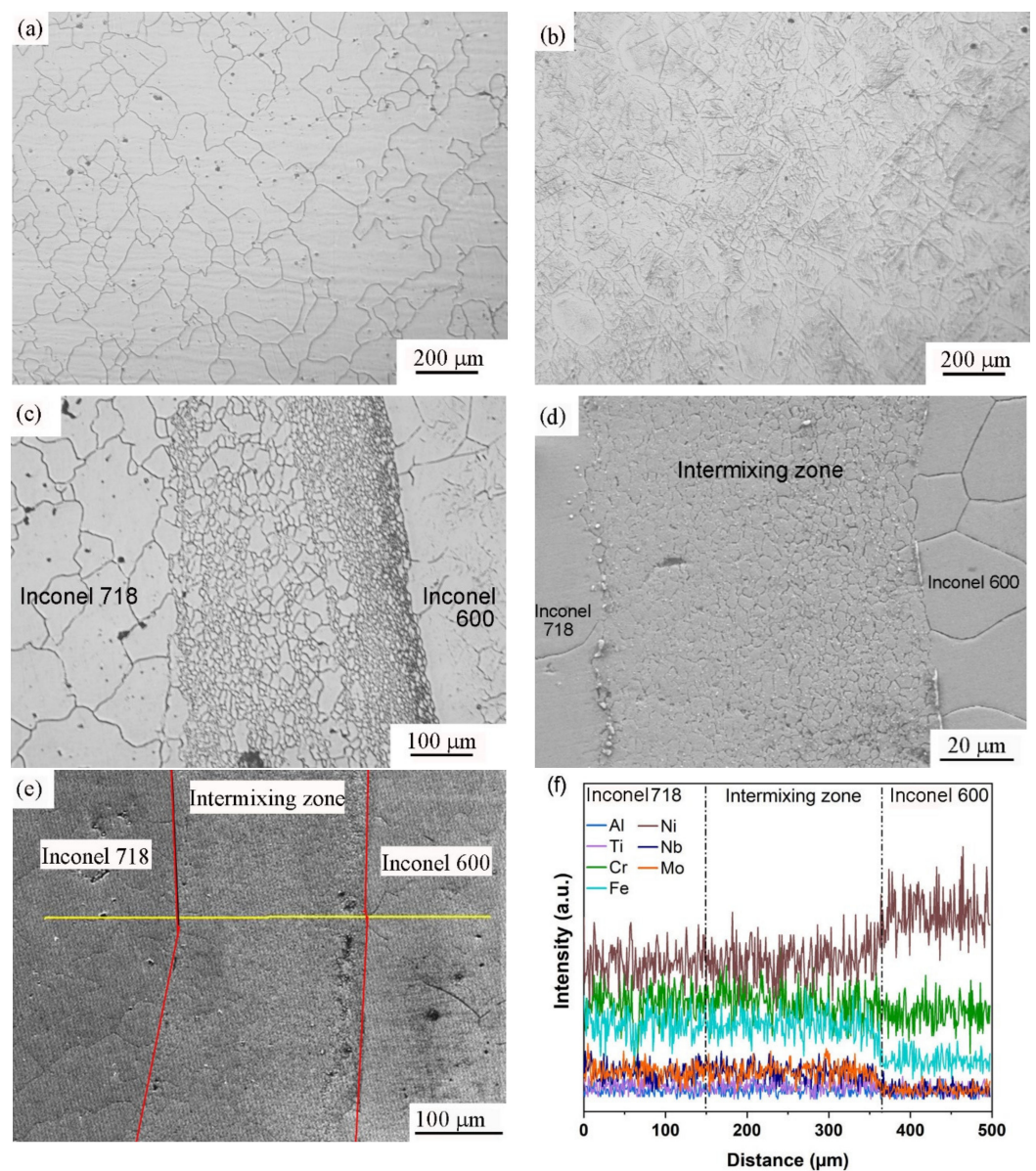


Figure 3. (a,b) heat effected zone (HAZ) micrographs of Inconel 718 and Inconel 600, respectively, showing grain coarsening. (c,d) optical and SEM micrographs of the weld interface, respectively. (e,f) results of the EDS line scan across the weld interface.

Figure 3c,d show the optical and SEM micrographs of the weld interface, respectively. As can be seen from the results of the EDS line scan (Figure 3e,f), the interface region showed some mechanical intermixing and very fine dynamically recrystallized grains. The width of this region was observed to vary from the weld center to the outer surface (the width was higher at the weld center, $\sim 300\text{ }\mu\text{m}$). Such a dynamically recrystallized region with some mechanical intermixing is typical of friction welds and is known to be caused by severe plastic deformation at high temperatures [20,21]. The average grain size in the mechanical intermixing zone was found to be $5.2 \pm 2.1\text{ }\mu\text{m}$. It can be seen from the EDS line scan data that the composition of the mechanical intermixing zone was close to the composition of the Inconel 718. This suggests that the Inconel 718 underwent plastic deformation to a greater extent compared with the Inconel 600 during friction welding. The absence of strengthening precipitates in solution treated Inconel 718 and the differences in weld thermal cycles experienced by the materials placed on the stationary and rotating sides during friction welding can account for this.

3.2. Mechanical Properties

Figure 4 shows the Vickers hardness profile across the dissimilar weld. The mechanical intermixing zone at the weld interface was observed to show high hardness, which can be attributed to its fine grain size (due to dynamic recrystallization during friction welding). The HAZ of the Inconel 718 showed considerably lower hardness compared with the Inconel 718 base metal. On the other hand, the HAZ of the Inconel 600 did not show any significant difference in hardness compared with the Inconel 600 base metal. The drop in HAZ hardness on the Inconel 718 side is attributable to significant grain coarsening. Furthermore, the low hardness in the HAZ of the Inconel 718 suggests that the thermal cycles involved in friction welding did not result in any precipitation of strengthening phases [22,23].

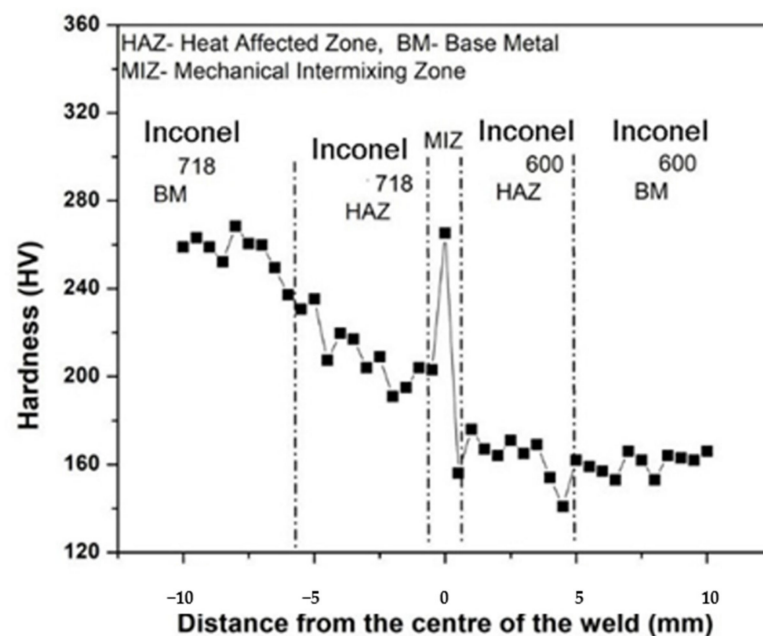


Figure 4. Vickers microhardness profile across the Inconel 718/Inconel 600 dissimilar friction weld.

Typical room temperature tensile plots of the two base metals and the dissimilar friction weld are shown in Figure 5. The average yield strength, ultimate tensile strength and % elongation values are presented in Table 3. Figure 6 shows that the failure location of the transverse tensile specimen corresponded to the dissimilar Inconel 600/Inconel 718 friction welded joint. All of the weld specimens were found to fail in the HAZ of the Inconel 718 close to the weld interface. The weld specimens showed lower yield and tensile

strengths compared with the Inconel 718 base metal. However, compared with the Inconel 600 base metal, the weld strength was not much inferior. With respect to % elongation, the weld specimens were inferior compared with both the Inconel 718 and the Inconel 600 base metals. The fracture surfaces of the Inconel 718 base metal, Inconel 600 base metal and Inconel 718/Inconel 600 dissimilar friction weld exhibited dimple features as can be seen in Figure 7a–c, respectively. Dimple fracture features suggest a ductile mode of fracture that occurred by nucleation and a growth of microvoids. These microvoids then joined together to produce larger voids until the remaining cross-sectional area of the tensile specimen became too small to support the applied load and finally a ductile fracture took place. It is interesting to note that the HAZ area of the Inconel 718 displayed good ductility in spite of the grain growth due to the thermal cycle experienced. Further studies involving post-weld ageing would be useful in analyzing the mechanical performance of Inconel 718/Inconel 600 dissimilar friction welds.

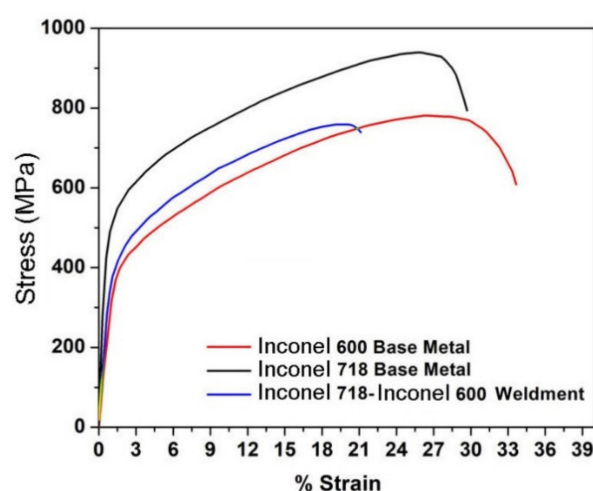


Figure 5. Typical engineering stress-strain curves of the Inconel 718 and Inconel 600 base metals and dissimilar friction welded joints.

Table 3. Results of room temperature tensile testing (average properties from three tests in each case).

Sample	Yield Strength (MPa)	Ultimate Tensile Strength (MPa)	Elongation (%)
Inconel 718 base metal	485 ± 7	940 ± 2	30 ± 2
Inconel 600 base metal	390 ± 8	780 ± 5	34 ± 1
Inconel 718/600 dissimilar friction weld	416 ± 10	759 ± 11	21 ± 4

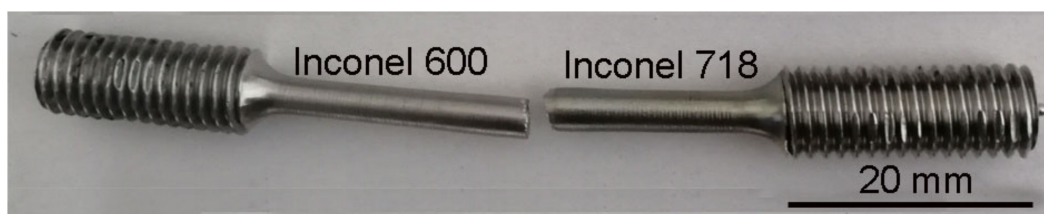


Figure 6. Failure location of the transverse tensile specimen corresponding to the dissimilar Inconel 600/Inconel 718 friction welded joint.

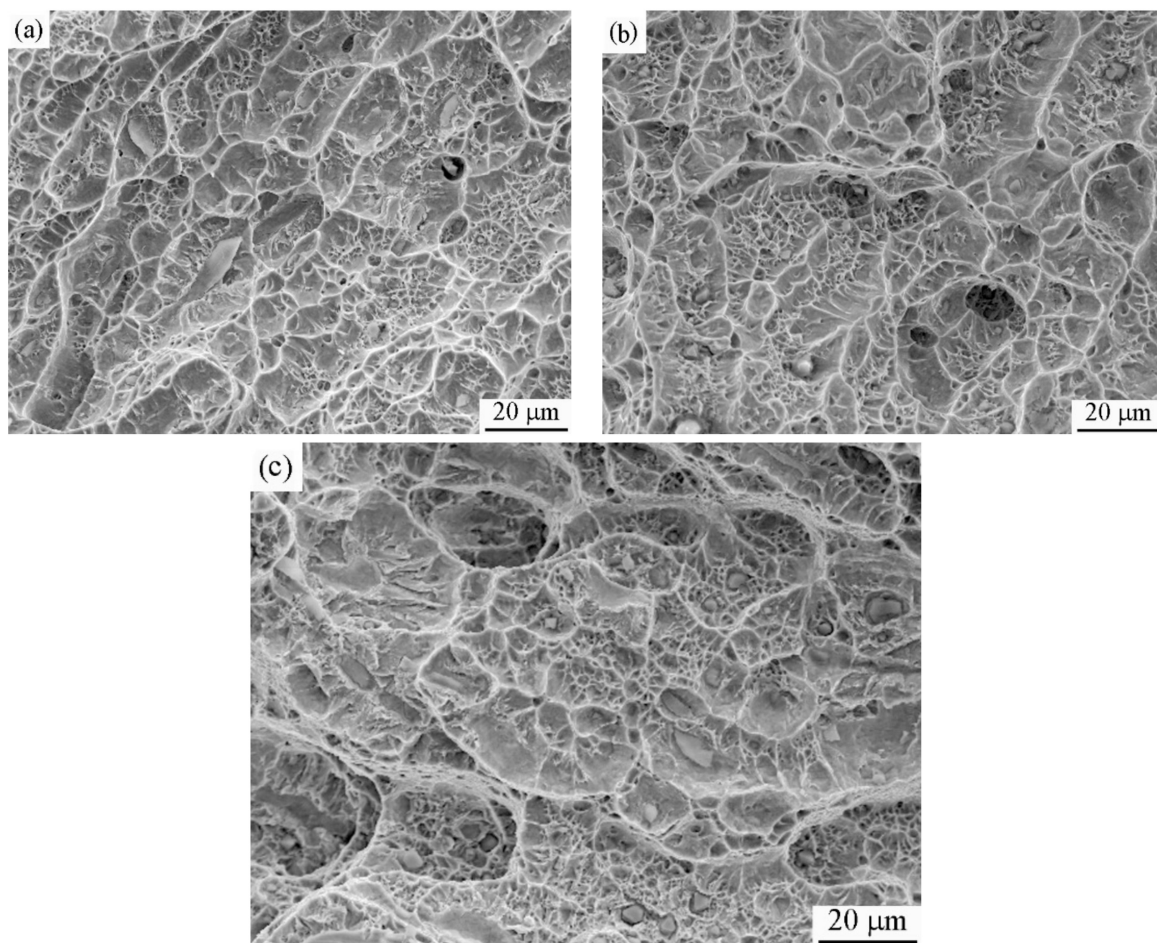


Figure 7. Tensile fracture surfaces: (a) Inconel 718 base metal, (b) Inconel 600 base metal, (c) Inconel 718/Inconel 600 dissimilar friction weld.

4. Conclusions

In this work, the rotary friction welding of solution treated Inconel 718 to mill annealed Inconel 600 was successfully carried out. Microstructural characteristics and room temperature tensile properties of the dissimilar friction welds were investigated. Based on the experimental findings, the following conclusions can be drawn:

- i. Friction welding can be readily used for joining Inconel 718 to Inconel 600. The welds did not suffer from major cracking problems. The welds were also free from undesirable elemental segregation and Laves formations.
- ii. No major undesirable microstructural changes took place in the HAZ of the Inconel 718 or Inconel 600 during friction welding. However, both of the alloys underwent some grain coarsening next to the weld interface.
- iii. The dissimilar weld was characterized by a narrow mechanical intermixing zone at the interface. In this zone, severe plastic deformation at high temperatures resulted in dynamic recrystallization leading to very fine equiaxed grains. Consequently, this zone displayed significantly higher hardness.
- iv. In an as-welded condition, Inconel 718/Inconel 600 dissimilar friction welds showed impressive room temperature tensile properties. The weld failed in the HAZ of the Inconel 718 due to significant grain coarsening.

Author Contributions: Conceptualization, A.U.R., Y.U., A.M.A.-S. and S.A.; methodology, A.U.R., Y.U., A.M.A.-S. and S.A.; formal analysis, A.U.R. and Y.U.; investigation, A.U.R., Y.U., A.M.A.-S. and S.A.; resources, A.U.R., Y.U., A.M.A.-S. and S.A.; writing—original draft preparation, A.U.R. and Y.U.; writing—review and editing, A.U.R., Y.U., A.M.A.-S. and S.A.; visualization, A.U.R. and S.A.;

supervision, A.U.R., A.M.A.-S. and S.A.; project administration, A.U.R. and Y.U.; funding acquisition, A.U.R. All authors have read and agreed to the published version of the manuscript.

Funding: This research was funded by the National Plan for Science, Technology and Innovation (MAARIFAH), King Abdulaziz City for Science and Technology, Kingdom of Saudi Arabia, Award Number (15-ADV3717-02).

Institutional Review Board Statement: Not applicable.

Informed Consent Statement: Not applicable.

Data Availability Statement: Data is contained within the article “Rotary Friction Welding of Inconel 718 to Inconel 600”.

Acknowledgments: This Project was funded by the National Plan for Science, Technology and Innovation (MAARIFAH), King Abdulaziz City for Science and Technology, Kingdom of Saudi Arabia, Award Number (15-ADV3717-02). The authors acknowledge Ashfaq Mohammad at the National Manufacturing Institute Scotland for his technical inputs during the experimental and writeup stages of the present work.

Conflicts of Interest: The authors declare no conflict of interest.

References

- Gorr, B.; Müller, F.; Azim, M.; Christ, H.J.; Müller, T.; Chen, H.; Kauffmann, A.; Heilmaier, M. High-Temperature Oxidation Behavior of Refractory High-Entropy Alloys: Effect of Alloy Composition. *Oxid. Met.* **2017**, *88*, 339–349. [CrossRef]
- Reed, R.C.; Rae, C.M.F. *Physical Metallurgy of the Nickel-Based Superalloys*, 5th ed.; Elsevier B.V.: Amsterdam, The Netherlands, 2014; Volume 1, ISBN 9780444537713.
- Bamford, W.; Hall, J. A Review of Alloy 600 Cracking in Operating Nuclear Plants Including Alloy 82 and 182 Weld Behavior. In Proceedings of the 12th International Conference on Nuclear Engineering, ICONE12-49520, Arlington, VA, USA, 25–29 April 2004; pp. 1–9.
- Sato, Y.S.; Arkom, P.; Kokawa, H.; Nelson, T.W.; Steel, R.J. Effect of Microstructure on Properties of Friction Stir Welded Inconel Alloy 600. *Mater. Sci. Eng. A* **2008**, *477*, 250–258. [CrossRef]
- Wang, C.; Li, R. Effect of Double Aging Treatment on Structure in Inconel 718 Alloy. *J. Mater. Sci.* **2004**, *39*, 2593–2595. [CrossRef]
- Lippold, J.C. *Welding Metallurgy and Weldability*; John Wiley & Sons, Inc.: Hoboken, NJ, USA, 2015; ISBN 9781118230701.
- Satyanarayana, V.V.; Reddy, G.M.; Mohandas, T. Dissimilar Metal Friction Welding of Austenitic-Ferritic Stainless Steels. *J. Mater. Process. Technol.* **2005**, *160*, 128–137. [CrossRef]
- Janaki Ram, G.D.; Venugopal Reddy, A.; Prasad Rao, K.; Reddy, G.M.; Sarin Sundar, J.K. Microstructure and Tensile Properties of Inconel 718 Pulsed Nd-YAG Laser Welds. *J. Mater. Process. Technol.* **2005**, *167*, 73–82. [CrossRef]
- Huang, X.; Chaturvedi, M.C.; Richards, N.L. An Investigation of Microstructure and HAZ Microfissuring of Cast Alloy 718. In Proceedings of the Superalloys 718, 625, 706 and Various Derivatives, San Diego, CA, USA, 20–23 September 1994; Loria, E.A., Ed.; The Minerals, Metals & Materials Society: Pittsburgh, PA, USA, 1994; pp. 871–880.
- Chamanfar, A.; Jahazi, M.; Cormier, J. A Review on Inertia and Linear Friction Welding of Ni-Based Superalloys. *Metall. Mater. Trans. A Phys. Metall. Mater. Sci.* **2015**, *46*, 1639–1669. [CrossRef]
- Kong, Y.S.; Cheepu, M.; Kim, D.G. Microstructure and Mechanical Properties of Friction-Welded and Post-Heat-Treated Inconel 718. *Trans. Indian Inst. Met.* **2020**, *73*, 1449–1453. [CrossRef]
- Damodaram, R.; Raman, S.G.S.; Rao, K.P. Microstructure and Mechanical Properties of Friction Welded Alloy 718. *Mater. Sci. Eng. A* **2013**, *560*, 781–786. [CrossRef]
- Smith, M.; Bichler, L.; Gholipour, J.; Wanjara, P. Mechanical properties and microstructural evolution of in-service Inconel 718 superalloy repaired by linear friction welding. *Int. J. Adv. Manuf. Technol.* **2017**, *90*, 1931–1946. [CrossRef]
- Liu, F.C.; Nelson, T.W. Grain structure evolution, grain boundary sliding and material flow resistance in friction welding of Alloy 718. *Mater. Sci. Eng. A* **2018**, *710*, 280–288. [CrossRef]
- Gobu, N.; Mahadevan, K. Evaluation of Mechanical and Metallurgical Properties of Friction Welded Inconel 600 and Aisi 304L Austenitic Stainless Steel Dissimilar Joints. *J. Manuf. Eng.* **2016**, *11*, 171–177. Available online: <http://smenec.org> (accessed on 5 December 2020).
- Rehman, A.U.; Babu, N.K.; Talari, M.K.; Usmani, Y.S.; Al-Khalefah, H. Microstructure and Mechanical properties of Dissimilar Friction Welding Ti-6Al-4V Alloy to Nitinol. *Metals* **2021**, *11*, 109. [CrossRef]
- Sims, C.T.; Stoloff, N.S.; Hagel, W.C. *Superalloys II: High Temperature Materials for Aerospace and Industrial Power*; Wiley Sons: Hoboken, NJ, USA, 1987.
- Knap, I.; Krawczyk, R. Temperature Measurement on the Interface of a Friction-Welded Joint. *Weld. Int.* **2000**, *14*, 964–969. [CrossRef]
- Devaux, A.; Nazé, L.; Molins, R.; Pineau, A.; Organista, A.; Guédou, J.Y.; Uginet, J.F.; Héritier, P. Gamma Double Prime Precipitation Kinetic in Alloy 718. *Mater. Sci. Eng. A* **2008**, *486*, 117–122. [CrossRef]

-
20. Murr, L.E.; Liu, G.; McClure, J.C. Dynamic Recrystallization in Friction-Stir Welding of Aluminium Alloy 1100. *J. Mater. Sci. Lett.* **1997**, *16*, 1801–1803. [[CrossRef](#)]
 21. Ahmed, M.M.Z.; Wynne, B.P.; Martin, J.P. Effect of Friction Stir Welding Speed on Mechanical Properties and Microstructure of Nickel Based Super Alloy Inconel 718. *Sci. Technol. Weld. Join.* **2013**, *18*, 680–687. [[CrossRef](#)]
 22. Anbarasan, N.; Gupta, B.K.; Prakash, S.; Muthukumar, P.; Oyyaravelu, R.; Kumar, R.J.F.; Jerome, S. Effect of Heat Treatment on the Microstructure and Mechanical Properties of Inconel 718. *Mater. Today Proc.* **2018**, *5*, 7716–7724. [[CrossRef](#)]
 23. Vincent, R. Precipitation around Welds in the Nickel-Base Superalloy, Inconel 718. *Acta Metall.* **1985**, *33*, 1205–1216. [[CrossRef](#)]